Journal of Alzheimer's Disease xx (20xx) x–xx
DOI 10.3233/JAD-200171
IOS Press

Classification of Alzheimer's Disease with Respect to Physiological Aging with Innovative EEG Biomarkers in a Machine Learning Implementation

Fabrizio Vecchio[a,*], Francesca Miraglia[a], Francesca Alù[a], Matteo Menna[a], Elda Judica[b], Maria Cotelli[c] and Paolo Maria Rossini[a]
[a]*Brain Connectivity Laboratory, Department of Neuroscience & Neurorehabilitation, IRCCS San Raffaele Pisana, Rome, Italy*
[b]*Department of Neurorehabilitation Sciences, Casa Cura Policlinico, Milano, Italy*
[c]*Neuropsychology Unit, IRCCS Istituto Centro San Giovanni di DioFatebenefratelli, Brescia, Italy*

Accepted 2 April 2020

Abstract.
Background: Several studies investigated clinical and instrumental differences to make diagnosis of dementia in general and in Alzheimer's disease (AD) in particular with the aim to classify, at the individual level, AD patients and healthy controls cooperating with neuropsychological tests for an early diagnosis. Advanced network analysis of electroencephalographic (EEG) rhythms provides information on dynamic brain connectivity and could be used in classification processes. If successfully reached, this goal would add a low-cost, easily accessible, and non-invasive technique with neuropsychological tests.
Objective: To investigate the possibility to automatically classify physiological versus pathological aging from cortical sources' connectivity based on a support vector machine (SVM) applied to EEG small-world parameter.
Methods: A total of 295 subjects were recruited: 120 healthy volunteers and 175 AD. Graph theory functions were applied to undirected and weighted networks obtained by lagged linear coherence evaluated by eLORETA. A machine-learning classifier (SVM) was applied. EEG frequency bands were: delta (2–4 Hz), theta (4–8 Hz), alpha1 (8–10.5 Hz), alpha2 (10.5–13 Hz), beta1 (13–20 Hz), beta2 (20–30 Hz), and gamma (30–40 Hz).
Results: The receiver operating characteristic curve showed AUC of 0.97 ± 0.03 (indicating very high classification accuracy). The classifier showed 95%±5% sensitivity, 96%±3% specificity, and 95%±3% accuracy for the classification.
Conclusion: EEG connectivity analysis via a combination of source/connectivity biomarkers, highly correlating with neuropsychological AD diagnosis, could represent a promising tool in identification of AD patients. This approach represents a low-cost and non-invasive method, one that utilizes widely available techniques which, when combined, reach high sensitivity/specificity and optimal classification accuracy on an individual basis (0.97 of AUC).

Keywords: Alzheimer's disease, delta and alpha bands, EEG, functional connectivity, graph theory, LORETA, machine learning classifier, small-world, support vector machine

INTRODUCTION

Alzheimer's disease (AD) is the most prevalent neurodegenerative disorder that accounts for more than 50–60% of all the dementia cases and affects

*Correspondence to: Fabrizio Vecchio, PhD, Brain Connectivity Laboratory, IRCCS San Raffaele Pisana, Via Val Cannuta, 247, 00166 Rome, Italy. Tel.: +39 06 52253767; E-mails: fabrizio.vecchio@uniroma1.it, fabrizio.vecchio@sanraffaele.it.

about 30% of all individuals of 85 years and above [1]. Aging is considered the most impacting and non-modifiable risk factor for almost all neurodegenerative diseases including AD. During aging, the human brain experiences a series of molecular, biochemical, structural. and functional changes [2], which can result in a greater susceptibility to disorders of brain functions mainly dealing with cognition (e.g., neurodegeneration, dementia including AD) [3]. Neurodegeneration is a pathological condition, mainly characterized by a progressive neuronal dysfunction, which represents a crucial trigger for a cascade of events initially affecting synaptic transmission and finally leading to neuronal death and the consequent loss of brain networks architecture.

Modelling the human brain as a complex network has provided a powerful mathematical framework to characterize its organization while aging processes and eventual neurodegeneration deviates from 'normality', the underlying brain network configuration. In the past decade, the combination of non-invasive neuroimaging techniques and graph theoretical approaches enable the mapping of human structural and functional connectivity patterns (i.e., connectome) at the macroscopic level. One of the most influential findings is that human brain networks exhibit prominent small-world (SW) organization. Such a network architecture in the human brain facilitates efficient information segregation and integration mainly based on frequency- and time-dependent synchronization and phase coherence of electroencephalographic oscillations (reflecting rhythmic firing of the neuronal assemblies) at low wiring and energy costs, which presumably results from natural selection under the pressure of a cost-efficiency balance. Moreover, the SW organization undergoes continuous changes during normal development and aging and exhibits dramatic alterations in different neurological disorders including the neurodegenerative ones [4–10]. Watts and Strogatz introduced the concept of the so-called 'small-world' networks, that allows an optimal balance between local specialization and global integration [11].

Several studies have previously investigated clinical and instrumental differences which, when combined with the neuropsychological tests, could help with early diagnosis of dementia in general and in AD in particular with the aim to classify and distinguish, at the individual level, AD patients from healthy controls. Several tools have been used, starting from structural or functional neurophysiological parameters such those extracted by magnetic resonance imaging (MRI)-functional MRI or electroencephalography (EEG). Several kinds of classifiers were designed. The more recent approach is to use modern machine learning methods.

These machine learning classifiers [12] provide a powerful approach to investigate differences in functional networks. One of the commonly used machine learning classifiers is support vector machine (SVM). A crucial aspect of SVM is that it identifies the features that drive classifier performance. An SVM algorithm trained on a training dataset can generate feature weights corresponding to the relative contribution of an individual feature to successful differentiation of two groups. Following this, the classifier can be applied to a separate testing dataset to assess the accuracy of the classifier in differentiating two groups.

The present study investigates the possibility to automatically classify physiological versus pathological brain aging, as clinically identified via an extensive battery of neuropsychological tests, from cortical sources' connectivity (by graph theory from exact low resolution brain electromagnetic tomography [eLORETA]) based on a SVM applied to EEG SW.

METHODS

Subjects

A total of 295 subjects were recruited from an available database. It consists of 175 AD patients (mean age = 73.2 ± 7.3 years, education = 7.1 ± 3.9 years, Mini-Mental State Examination [MMSE] = 20 ± 4) and 120 healthy aging volunteers (mean age = 72.1 ± 7.2 years, education = 9.3 ± 4.3 years, MMSE = 28.4 ± 1.4). Exclusion criteria for healthy volunteers included a history of neurological or psychiatric disorder, or current treatment with vasoactive or psychotropic medication. All subjects were right-handed based on the Handedness Questionnaire [13].

AD subjects were diagnosed according to the National Institute on Aging-Alzheimer's Association workgroups [14] and DSM IV TR criteria. Moreover, they showed reduction in the volume of hippocampus and increased width of the temporal horn and of the choroidal fissure [15].

Exclusion criteria for AD included any evidence of 1) frontotemporal dementia, diagnosed according to criteria of Lund and Manchester Groups (1994), 2) vascular dementia, diagnosed according to NINDS-

AIREN criteria [16], 3) extra-pyramidal syndromes, 4) reversible dementias (including pseudodementia of depression); and 5) Lewy body dementia, according to the criteria by [17].

The study was approved by local Ethical Committee. Experimental procedures were conformed to the Declaration of Helsinki and national guidelines.

Data recordings and preprocessing

The EEG recordings of each subject were carried out with several EEG machines, as this was a multicentric study, with 19 or 32 electrodes positioned according with the International 10–20 system. Two separate channels, vertical and horizontal EOGs, were used to monitor eyes movements and blinking. Impedance was kept below 10 KΩ and the sampling rate frequency was set up at least at 256 Hz. Electroencephalographic signals were measured at rest, in at least 5 min of closed eyes and no task conditions. During the recording, subjects were seated and relaxed in a sound attenuated and dimly lit room.

The data were processed in Matlab (MathWorks, Natick, MA) using scripts based on EEGLAB toolbox (Swartz Center for Computational Neurosciences, La Jolla, CA; http://www.sccn.ucsd.edu/eeglab) .

The EEG recordings were band-pass filtered from 0.2 to 47 Hz using a finite impulse response (FIR) filter. Imported data were divided in 2 s duration epochs and principal artifacts in the EEG recordings (i.e., eye movements, cardiac activity, and scalp muscle contraction) were removed with Infomax ICA algorithm [18] that enables the separation of statistically independent sources from multichannel EEG recordings [19–21], as implemented in the EEGLAB.

Functional connectivity analysis

Brain connectivity was computed by eLORETA software on 84 ROIs defined according to the 42 Brodmann areas, for the left and right hemispheres. ROIs are needed for the estimation of electric neuronal activity that is used to analyze brain functional connectivity.

Among the eLORETA current density time series of the 84 ROIs, intracortical Lagged Linear Coherence, extracted by "all nearest voxels" method [22, 23], was computed between all possible pairs of the 84 ROIs for each of the seven independent EEG frequency bands [24, 25] of delta (2–4 Hz), theta (4–8 Hz), alpha 1 (8–10.5 Hz), alpha 2 (10.5–13 Hz), beta 1 (13–20 Hz), beta 2 (20–30 Hz), and gamma (30–45 Hz), for each subject.

Lagged linear coherence was developed as a measure of true physiological connectivity not affected by volume conduction and low spatial resolution. The values of connectivity computing between all pairs of regions of interest (ROIs) for each frequency band and for each subject, were used as measure of weight of the graph in the follow graph analyses.

Graph analysis

A network is a mathematical representation of a complex system and is defined by a collection of nodes (vertices) and links (edges) between pairs of nodes [26, 27]. When network representation is applied to a brain model from EEG signals, nodes represent cortical areas, while edges could be directed or undirected, unweighted or weighted with measures of functional or effective connectivity between nodes.

In this study, weighted and undirected networks were built with Brain Connectivity Toolbox, adapted with our own Matlab scripts. The vertices of the network were the estimated cortical sources in the BAs, and the edges were weighted by the lagged linear values within each pair of vertices [28].

SW parameter was evaluated on brain networks, since it measures the balance between local connectedness and global integration of a network, representing brain network organization. SW organization is intermediate between that of random networks, the short overall path length of which is associated with a low level of local clustering, and that of regular networks or lattices, the high-level of clustering of which is accompanied by a long path length. The measure of network small-worldness was defined as the ratio of the normalized clustering coefficient Cw, and the normalized path length Lw [29, 30] in all the EEG bands.

Support vector machine

Classifier description and creation

The addressed problem was to estimate the AD probability given a set of features $F = \{f_1, \ldots, f_n\}$, namely the data coming from SW values for delta, theta, alpha 1, alpha 2, beta 1, beta 2, and gamma. The problem has been hence brought back to estimate a binary classifier $y(F)\colon \mathbb{R}^n \rightarrow \{0, \ldots, 1\}$, where 0 means healthy and 1 is AD.

The proposal approach is composed by three phases: features standardization, features dimension-

ality reduction through principal component analysis (PCA), and input classification using an SVM. The aim of the first two phase is to preprocess the data and make easier the solution of the classification problem.

Standardization

It is a procedure to convert a random variable, distributed with mean μ and variance σ^2, into a random variable with "standard" distribution, namely with zero mean and standard deviation equal to 1. Therefore, each feature f_i is transformed in $z_i = \frac{f_i - \mu_i}{\sigma_i}$ [31]. The main advantage of standardization is to avoid attributes in greater numeric ranges dominating those in smaller numeric ranges. Another advantage is to avoid numerical difficulties during the computation. Indeed, since kernel values depend on the inner products of feature vectors, large attribute values might cause numerical problems.

PCA

PCA is a dimensionality reduction technique used to map the features to a lower-dimensional space. PCA is a technique for reducing the dimensionality of the datasets, increasing interpretability but at the same time minimizing information loss. It does so by creating new uncorrelated variables that successively maximize variance. Finding such new variables, the principal components, reduces to solving an eigenvalue/eigenvector problem, and the new variables are defined by the dataset at hand, not *a priori*, hence making PCA an adaptive data analysis technique.

This result is obtained by applying an orthogonal transformation projecting linear dependent features in to linear independent variables and select among the latter the components that store more information in the form of variants. PCA are widely used in literature for dataset processioning [32].

PCA is applied after the standardization step as described above, so the features vector $F = \{f_1, f_2, \ldots, f_N\}$ has been transformed to the standard feature vector $Z = \{z_1, z_2, \ldots, z_N\}$ applying [31].

PCA technique operate as follow:

1. Compute co-variance matrix Σ where the element (i, j) of Σ is the co-variance:

$$K_{Z_i Z_j} = cov[Z_i, Z_j] = E[(Z_i - E[Z_i])(Z_j - E[Z_j])]$$

2. Factorization of the co-variance matrix in canonical form: $\Sigma = Q \Lambda Q^{-1}$ where Q is the matrix composed by the eigenvectors of Σ and Λ is a diagonal matrix where each element of the main diagonal λ is an eigenvalue of Σ.

3. Feature projection in to the sub-space composed by the eigenvector associated with the eigenvalues that describe the 80% of the total variance: $\sum_{i=1}^{M<N} \lambda_i = 0.8$. The choice of the PCA threshold of 0.8 has been found in an empirical way. We iteratively increased the threshold from 0.1 to 0.9 and selected the value for which the best performance on the test set was obtained. (See Results for more details). Figure 1 shows the results of the different iteration. The grey area represents the confidence level at 95%.

Table 1 summarizes the results of PCA analyses applied to our dataset. The table shows the eigenvectors that define the new hyperspace, namely the matrix Q. Every row is a new component. The table also show the contribution from every dimension in the original space, the SW features, to every new component.

Table 2 shows the value of the eigenvalues, namely the elements from diagonal matrix Λ. The firs eigenvalue $\lambda_1 = 0.352$ is the eigenvalue associated with the eigenvector pca1. This means that the eigen vector

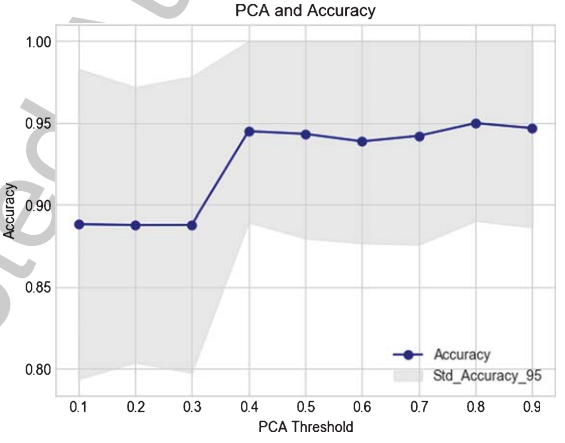

Fig. 1. Results of different iterations. The grey area represents the confidence level at 95%.

Table 1
Results of PCA analyses applied to our dataset

	delta	Theta	alpha 1	alpha 2	beta 1	beta 2	gamma
pca_1	0.1877	0.0134	–0.4809	–0.3246	0.2765	0.5534	0.4950
pca_2	0.4874	0.6290	0.0607	0.47140	0.3251	–0.1686	–0.0819
pca_3	0.6282	–0.1209	–0.4878	0.4374	0.1399	–0.1323	–0.3523
pca_4	–0.1666	0.4151	0.0859	–0.0968	0.8160	–0.0395	0.3398
pca_5	0.4068	–0.5964	0.3957	–0.4524	0.2840	0.1917	0.005
pca_6	0.2429	0.2362	0.2969	0.4389	0.2210	–0.2951	0.6843
pca_7	–0.2831	–0.0752	–0.5242	–0.272	0.0517	–0.7226	0.2003

Table 2
Value of the eigenvalues

λ_1	λ_2	λ_3	λ_4	λ_5	λ_6	λ_7
0.352	0.225	0.139	0.1211	0.079	0.048	0.036

pca1 is a direction that explains the 35.2% of the total dataset variance. And so on for the other components.

The PCA result is summarized by:

$$PCA(Z) = X = \{x_1, \ldots, x_m\}$$

SVM

The features obtained by dimensionality reduction through PCA described above are used to train a binary classifier based on SVM.

The SVM is a hyperplane, or a set of hyperplanes, that can be used to classify a new input. Intuitively a good separation between classes is composed by the hyperplane with higher distance (called margin), from a point in the dataset belonging to each class, since in general the greater the margin the lower the classification error.

Given a vector $X = \{x_1, \ldots, x_M\}$ and the correspondent output $y \in \{-1, 1\}^M$, the SVM solves the problem:

$$\min_{w.b.\zeta} \frac{1}{2} w^T w + C \sum_{i=1}^{n} (\zeta_i)$$

$$subject\ to\ y_i(w^T \phi(x_i) + b) \geqslant 1 - \zeta_i,$$

$$\zeta_i \geq 0, i = 1, \ldots, n$$

Its dual is

$$\min_{\alpha} \frac{1}{2} \alpha^T Q \alpha - e^T \alpha$$

$$subject\ to\ y^T \alpha = 0,$$

$$0 \leqslant \alpha \leqslant C, i = 1, \ldots, n$$

where e is the all one vector, $C>0$ is the upper bound, Q is a matrix n x n positive and semi-definite, $Q_{ij} = y_i y_j K(x_i, x_j)$, where $K(x_i, x_j) = \phi(x_i)^T \phi(x_j)$ is a kernel function. In this implementation, the kernel is the radial basis function $K(x, x^t) = \exp\left(\frac{-\|x-x\|^2}{2\sigma^2}\right)$ and σ is estimated with Maximum Likelihood.

Solving the dual problem, we obtained the solution:

$$f(x) = sgn\left(\sum_{i=1}^{n} y_i\, \alpha K(x_i, x) + \rho\right)$$

given a new input x the function f returns a value y between –1 and 1. To guarantee a value between 0 and 1 y is normalized using: $(y + 1)/2$

We used the implementation contained in the open source library *Scikit-learn: Machine Learning in Python.*

Training and evaluation

The standard approach in machine-learning environment in order to train and evaluate a statistical model is to randomly split the dataset in training set and test set. The training set is used to train the model. This means that the model sees and learns only from this data set that defines the error function minimized during training as explained in the previous section. The test set is used to evaluate model performances, classification accuracy in our case.

In order to have a complete and exhaustive model evaluation, we followed a cross validation technique: the dataset is iteratively and randomly split in 80% train set and 20% test set for 100 times. At each iteration, the model is trained making use of the train set and the accuracy is computed on the test set. The final accuracy is computed as the average of accuracy for all the iteration. In order to assess variance between the different iteration, we also compute the standard deviation. We follow a similar approach to compute sensitivity, specificity, area under the curve (AUC), and receiver operating characteristic (ROC) curve (Fig. 2).

RESULTS

In the classification process considering the seven SW values (i.e., SW index computed in delta, theta, alpha 1, alpha 2, beta 1, beta 2, gamma frequency EEG bands), the ROC (red line in Fig. 2) curve showed an AUC of 0.97 ± 0.03 (indicating very high classification accuracy). The resulting classifier showed $95\% \pm 5\%$ sensitivity, $96\% \pm 3\%$ specificity, and $95\% \pm 3\%$ accuracy for the classification of the AD respect to control subjects.

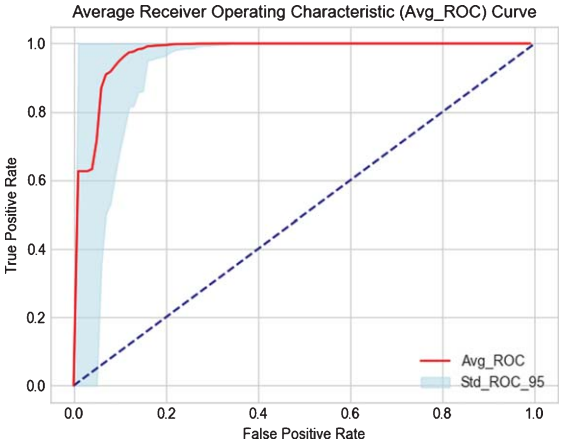

Fig. 2. Average receiver operating characteristic (ROC) curves and their confidence intervals, illustrating the classification of the individual based small-world (red line). The area under the ROC (AUC) curves was 0.97 (std = 0.04), indicating an optimal classification accuracy.

DISCUSSION

EEG characteristics are known to change across physiological and pathological aging (especially due to neurodegeneration), with gradual modifications in spectral power profile indicating (in awake, resting conditions) a pronounced amplitude decrease of alpha and a global "slowing" of the background EEG rhythms, with increase in power and topography in the slower delta and theta frequencies. Such degenerative processes leading to EEG profile modulation are due to changes of sources and network configuration of brain connectivity as revealed by modern graph analyses [33–36].

Here we evaluated the possibility to automatically classify physiological versus pathological brain aging from cortical sources' connectivity (by graph theory from eLORETA) based on an SVM applied to EEG SW index. The current results suggested that our classifier is able to distinguish AD (as defined on the basis of neuropsychological, clinically validated, and standardized criteria) with respect to control subjects with a ROC curve showing an AUC of 0.97 ± 0.03 (indicating very high classification accuracy). The resulting classifier showed 95%±5% sensitivity, 96%±3% specificity, and 95%±3% accuracy for the classification of the AD respect to control subjects.

Very few studies are trying to evaluate differences for an early diagnosis of dementia [37]. A recent study also illustrates normative data of this SW parameter [3] underlining the always increased importance of this parameter.

Furthermore, several studies have previously investigated clinical and instrumental differences in order to combine them (or even to replace) with the standard neuropsychological tests for early diagnosis of dementia in general and of AD in particular with the aim to classify, at individual level, AD patients and healthy controls. Several tools have been used, such as diffusion MRI, with an AUC of 0.896 [38] or the combination of MRI and ROIs based classification that showed an AUC of 0.954 for classification and an accuracy of 89.63% [39].

Over time, efforts have been made to use less invasive, financially sustainable, and widely affordable techniques for the discrimination of AD patients such as EEG. For example, in a recent study, cortical sources of power and functional connectivity of EEG rhythms showed a sensitivity of 73.3%, specificity of 78%, accuracy of 75.5%, and AUC of 82% [40]. Power spectral density values with an SVM showed an accuracy of 84.4%, sensitivity 75.0%, and specificity of 93.7% [41]. Absolute and relative spectral power, distribution of spectral power, and measures of spatial synchronization studied with a SVM showed values of 89% and 88% for sensitivity and specificity [42]. A regression model combining cognitive data and quantitative EEG measurements provided an accuracy of 95.3% in the classification [43]; also, sensitivity of EEG and the combination of regional cerebral blood flow examination was 88% and specificity 89%, with a total accuracy of 88.3 [44].

The discriminatory power of quantitative EEG applying the statistical pattern recognition method showed an AUC of 0.90, a sensitivity of 84%, and a specificity of 81% [45], or the combination of a quantitative EEG method with specific neuropsychophysical tests presented a 94% of specificity and 88% of sensitivity [46]. The surface topography of the multivariate phase synchronization of multichannel EEG discriminates patients with an accuracy of up to 94% [47]. Auditory event-related P300 mainly generated in temporoparietal regions reached sensitivity of 86.7% and specificity of 76.7% [48]. The amplitude and 3-dimensional localization of equivalent EEG sources, evaluated using fast Fourier transform dipole and global field power, showed 84% correct classification [49].

Finally, several nonlinear signal complexity measures such as Higuchi fractal dimension, spectral entropy, spectral centroid, spectral roll-off, and zero-crossing rate combining with training of an SVM

resulted in a diagnostic accuracy of 78% [50]; quadratic sample entropy accuracy 77.27% and AUROC was more than 80% [51].

Also, a novel entropy measure, termed epoch-based entropy that quantifies disorder of EEG signals both at the time and spatial levels, using local density estimation by a Hidden Markov Model on inter-channel stationary epochs, reached a classification accuracy of 83%, specificity of 83.3%, and sensitivity of 82.3% [52]. Also fractal dimension is used for the evaluation of the dynamical changes in the AD brain, such as Katz fractal dimension, in particular on the global Katz fractal dimension in the β-band of the eyes-closed condition that showed an high accuracy of 99.3% with a sensitivity of 100% and a specificity of 97.8% [53].

To the best of our knowledge, this is the first study in which EEG graph theory parameters are used to classify AD patients with respect to healthy subjects. Is the "graph theoretical" model superior to other types of EEG analysis in an AD diagnostic context? It is not easy to answer this question; reading the most recent literature, it is evident there is an increasing number of studies addressing the idea to evaluate the optimal individual classifier to distinguish between AD and age-matched healthy subjects.

It is evident that brain characteristics are modulated by neurodegeneration and that this pathological condition alters brain network wiring and architecture with a severe impact on brain functions, particularly in the cognitive domains. Brain connectivity involves networks of regions directly linked via anatomical tracts or by functional associations. Brain networks are invariably complex, share a number of common features with networks from other biological and physical systems, and may hence be characterized by using complex network methods of analysis. The concept of functional connectivity is viewed as pivotal for understanding the organized behavior of neuronal networks during brain activity. This organization is probably based on the dynamic and time-varying interaction between different and variably specialized cortical sites. Cortical functional connectivity estimate aims at describing these interactions as connectivity patterns, which reflect strength of the information flow amongst the involved cortical areas.

The intrinsic characteristics of EEG rhythms on brain networks could contain relevant information on neurodegenerative processes underlying AD and the present work opens new avenues for the use of this kind of low-cost, non-invasive, and widely available biomarker for the classification of patients.

Conclusions

Graph theory analysis of brain connectivity from EEG signals provide useful information in distinguishing physiological and pathological age-related brain processes. In conclusion, EEG connectivity analysis via a combination of source/connectivity biomarkers could represent promising tool in the identification of AD patients also as a low-cost, non-invasive, and widely available screening method for large population samples reaching extremely high sensitivity/specificity and good classification accuracy on an individual basis (higher than 0.97 of AUC).

ACKNOWLEDGMENTS

This work was partially supported by the Italian Ministry of Health for Institutional Research (Ricerca corrente) and for the project "NEUROMASTER: NEUROnavigated MAgnetic STimulation in patients with mild-moderate Alzheimer disease combined with Effective cognitive Rehabilitation" (GR-2013-02358430).

Authors' disclosures available online (https://www.j-alz.com/manuscript-disclosures/20-0171r1).

REFERENCES

[1] Graham WV, Bonito-Oliva A, Sakmar TP (2017) Update on Alzheimer's disease therapy and prevention strategies. *Annu Rev Med* **68**, 413-430.

[2] Trollor JN, Valenzuela MJ (2001) Brain ageing in the new millennium. *Aust N Z J Psychiatry* **35**, 788-805.

[3] Vecchio F, Miraglia F, Judica E, Cotelli M, Alù F, Rossini PM (2020) Human brain networks: A graph theoretical analysis of cortical connectivity normative database from EEG data in healthy elderly subjects. *Geroscience*, doi: 10.1007/s11357-020-00176-2.

[4] Bassett DS, Bullmore E (2006) Small-world brain networks. *Neuroscientist* **12**, 512-523.

[5] Bullmore E, Sporns O (2009) Complex brain networks: Graph theoretical analysis of structural and functional systems. *Nat Rev Neurosci* **10**, 186-198.

[6] Bullmore E, Sporns O (2012) The economy of brain network organization. *Nat Rev Neurosci* **13**, 336-349.

[7] He Y, Evans A (2010) Graph theoretical modeling of brain connectivity. *Curr Opin Neurol* **23**, 341-350.

[8] Park HJ, Friston K (2013) Structural and functional brain networks: From connections to cognition. *Science* **342**, 1238411.

[9] Reijneveld JC, Ponten SC, Berendse HW, Stam CJ (2007) The application of graph theoretical analysis to complex networks in the brain. *Clin Neurophysiol* **118**, 2317-2331.

[10] Craddock M, Martinovic J, Müller MM (2013) Task and spatial frequency modulations of object processing: An EEG study. *PLoS One* **8**, e70293.

[11] Watts DJ, Strogatz SH (1998) Collective dynamics of 'small-world' networks. *Nature* **393**, 440-442.

[12] Pereira F, Mitchell T, Botvinick M (2009) Machine learning classifiers and fMRI: A tutorial overview. *Neuroimage* **45**, S199-209.

[13] Salmaso D, Longoni AM (1985) Problems in the assessment of hand preference. *Cortex* **21**, 533-549.

[14] McKhann GM, Knopman DS, Chertkow H, Hyman BT, Jack CR, Kawas CH, Klunk WE, Koroshetz WJ, Manly JJ, Mayeux R, Mohs RC, Morris JC, Rossor MN, Scheltens P, Carrillo MC, Thies B, Weintraub S, Phelps CH (2011) The diagnosis of dementia due to Alzheimer's disease: Recommendations from the National Institute on Aging-Alzheimer's Association workgroups on diagnostic guidelines for Alzheimer's disease. *Alzheimers Dement* **7**, 263-269.

[15] Wahlund LO, Julin P, Johansson SE, Scheltens P (2000) Visual rating and volumetry of the medial temporal lobe on magnetic resonance imaging in dementia: A comparative study. *J Neurol Neurosurg Psychiatry* **69**, 630-635.

[16] Román GC, Tatemichi TK, Erkinjuntti T, Cummings JL, Masdeu JC, Garcia JH, Amaducci L, Orgogozo JM, Brun A, Hofman A, Moody DM, O'Brien MD, Yamaguchi T, Grafman J, Drayer BP, Bennett DA, Fisher M, Ogata J, Kokmen E, Bermejo F, Wolf PA, Gorelick PB, Bick KL, Pajeau AK, Bell MA, DeCarli C, Culebras A, Korczyn AD, Bogousslavsky J, Hartmann A, Scheinberg P (1993) Vascular dementia: Diagnostic criteria for research studies. Report of the NINDS-AIREN International Workshop. *Neurology* **43**, 250-260.

[17] McKeith IG, Perry EK, Perry RH (1999) Report of the second dementia with Lewy body international workshop: Diagnosis and treatment. Consortium on Dementia with Lewy Bodies. *Neurology* **53**, 902-905.

[18] Bell AJ, Sejnowski TJ (1995) An information-maximization approach to blind separation and blind deconvolution. *Neural Comput* **7**, 1129-1159.

[19] Hoffmann S, Falkenstein M (2008) The correction of eye blink artefacts in the EEG: A comparison of two prominent methods. *PLoS One* **3**, e3004.

[20] Iriarte J, Urrestarazu E, Valencia M, Alegre M, Malanda A, Viteri C, Artieda J (2003) Independent component analysis as a tool to eliminate artifacts in EEG: A quantitative study. *J Clin Neurophysiol* **20**, 249-257.

[21] Jung TP, Makeig S, Humphries C, Lee TW, McKeown MJ, Iragui V, Sejnowski TJ (2000) Removing electroencephalographic artifacts by blind source separation. *Psychophysiology* **37**, 163-178.

[22] Pascual-Marqui RD, Lehmann D, Koukkou M, Kochi K, Anderer P, Saletu B, Tanaka H, Hirata K, John ER, Prichep L, Biscay-Lirio R, Kinoshita T (2011) Assessing interactions in the brain with exact low-resolution electromagnetic tomography. *Philos Trans A Math Phys Eng Sci* **369**, 3768-3784.

[23] Pascual-Marqui RD (2007) Instantaneous and lagged measurements of linear and nonlinear dependence between groups of multivariate time series: Frequency decomposition. arXiv, 0711.1455.

[24] Kubicki S, Herrmann WM, Fichte K, Freund G (1979) Reflections on the topics: EEG frequency bands and regulation of vigilance. *Pharmakopsychiatr Neuropsychopharmakol* **12**, 237-245.

[25] Niedermeyer E, Lopes da Silva F (1993) *Electroencephalography, Basic Principles, Clinical Applications and Related Fields*. Oxford University Press.

[26] Vecchio F, Miraglia F, Maria Rossini P (2017) Connectome: Graph theory application in functional brain network architecture. *Clin Neurophysiol Pract* **2**, 206-213.

[27] Miraglia F, Vecchio F, Rossini PM (2018) Brain electroencephalographic segregation as a biomarker of learning. *Neural Netw* **106**, 168-174.

[28] Vecchio F, Miraglia F, Rossini PM (2019) Tracking neuronal connectivity from electric brain signals to predict performance. *Neuroscientist* **25**, 86-93.

[29] Rubinov M, Sporns O (2010) Complex network measures of brain connectivity: Uses and interpretations. *Neuroimage* **52**, 1059-1069.

[30] Vecchio F, Miraglia F, Quaranta D, Lacidogna G, Marra C, Rossini PM (2018) Learning processes and brain connectivity in a cognitive-motor task in neurodegeneration: Evidence from EEG network analysis. *J Alzheimers Dis* **66**, 471-481.

[31] Guyon I, Boser B, Vapnik V (1993) Automatic capacity tuning of very large VC-dimension classifiers. *Advances in Neural Information Processing Systems* 5, [NIPS Conference], November 1992, 147–155.

[32] Ramírez-Gallego S, Krawczyk B, García S, Woźniak M, Herrera F (2017) A survey on data preprocessing for data stream mining: Current status and future directions. *Neurocomputing* **239**, 39-57.

[33] Vecchio F, Miraglia F, Marra C, Quaranta D, Vita MG, Bramanti P, Rossini PM (2014) Human brain networks in cognitive decline: A graph theoretical analysis of cortical connectivity from EEG data. *J Alzheimers Dis* **41**, 113-127.

[34] Vecchio F, Miraglia F, Bramanti P, Rossini PM (2014) Human brain networks in physiological aging: A graph theoretical analysis of cortical connectivity from EEG data. *J Alzheimers Dis* **41**, 1239-1249.

[35] Vecchio F, Miraglia F, Iberite F, Lacidogna G, Guglielmi V, Marra C, Pasqualetti P, Tiziano FD, Rossini PM (2018) Sustainable method for Alzheimer dementia prediction in mild cognitive impairment: Electroencephalographic connectivity and graph theory combined with apolipoprotein E. *Ann Neurol* **84**, 302-314.

[36] Miraglia F, Vecchio F, Rossini PM (2017) Searching for signs of aging and dementia in EEG through network analysis. *Behav Brain Res* **317**, 292-300.

[37] Rossini PM, Cappa SF, Lattanzio F, Perani D, Spadin P, Tagliavini F, Vanacore N (2019) The Italian INTERCEPTOR Project: From the early identification of patients eligible for prescription of antidementia drugs to a nationwide organizational model for early Alzheimer's disease diagnosis. *J Alzheimers Dis* **72**, 373-388.

[38] Schouten TM, Koini M, Vos F, Seiler S, Rooij M, Lechner A, Schmidt R, Heuvel MVD, Grond JV, Rombouts SARB (2017) Individual classification of Alzheimer's disease with diffusion magnetic resonance imaging. *Neuroimage* **152**, 476-481.

[39] Liu J, Li M, Lan W, Wu FX, Pan Y, Wang J (2018) Classification of Alzheimer's disease using whole brain hierarchical network. *IEEE/ACM Trans Comput Biol Bioinform* **15**, 624-632.

[40] Babiloni C, Triggiani AI, Lizio R, Cordone S, Tattoli G, Bevilacqua V, Soricelli A, Ferri R, Nobili F, Gesualdo L, Millán-Calenti JC, Buján A, Tortelli R, Cardinali V, Barulli MR, Giannini A, Spagnolo P, Armenise S, Buenza G, Scianatico G, Logroscino G, Frisoni GB, Del Percio C (2016) Classification of single normal and alzheimer's disease indi-

viduals from cortical sources of resting state EEG rhythms. *Front Neurosci* **10**, 47.

[41] Aghajani H, Zahedi E, Jalili M, Keikhosravi A, Vahdat BV (2013) Diagnosis of early Alzheimer's disease based on EEG source localization and a standardized realistic head model. *IEEE J Biomed Health Inform* **17**, 1039-1045.

[42] Lehmann C, Koenig T, Jelic V, Prichep L, John RE, Wahlund LO, Dodge Y, Dierks T (2007) Application and comparison of classification algorithms for recognition of Alzheimer's disease in electrical brain activity (EEG). *J Neurosci Methods* **161**, 342-350.

[43] Fonseca LC, Tedrus GM, Fondello MA, Reis IN, Fontoura DS (2011) EEG theta and alpha reactivity on opening the eyes in the diagnosis of Alzheimer's disease. *Clin EEG Neurosci* **42**, 185-189.

[44] Rodriguez G, Nobili F, Rocca G, De Carli F, Gianelli MV, Rosadini G (1998) Quantitative electroencephalography and regional cerebral blood flow: Discriminant analysis between Alzheimer's patients and healthy controls. *Dement Geriatr Cogn Disord* **9**, 274-283.

[45] Engedal K, Snaedal J, Hoegh P, Jelic V, Bo Andersen B, Naik M, Wahlund LO, Oeksengaard AR (2015) Quantitative EEG applying the statistical recognition pattern method: A useful tool in dementia diagnostic workup. *Dement Geriatr Cogn Disord* **40**, 1-12.

[46] Sneddon R, Shankle WR, Hara J, Rodriquez A, Hoffman D, Saha U (2005) EEG detection of early Alzheimer's disease using psychophysical tasks. *Clin EEG Neurosci* **36**, 141-150.

[47] Knyazeva MG, Jalili M, Brioschi A, Bourquin I, Fornari E, Hasler M, Meuli R, Maeder P, Ghika J (2010) Topography of EEG multivariate phase synchronization in early Alzheimer's disease. *Neurobiol Aging* **31**, 1132-1144.

[48] Juckel G, Clotz F, Frodl T, Kawohl W, Hampel H, Pogarell O, Hegerl U (2008) Diagnostic usefulness of cognitive auditory event-related p300 subcomponents in patients with Alzheimers disease? *J Clin Neurophysiol* **25**, 147-152.

[49] Huang C, Wahlund L, Dierks T, Julin P, Winblad B, Jelic V (2000) Discrimination of Alzheimer's disease and mild cognitive impairment by equivalent EEG sources: A cross-sectional and longitudinal study. *Clin Neurophysiol* **111**, 1961-1967.

[50] Staudinger T, Polikar R (2011) Analysis of complexity based EEG features for the diagnosis of Alzheimer's disease. *Conf Proc IEEE Eng Med Biol Soc* **2011**, 2033-2036.

[51] Simons S, Abasolo D, Escudero J (2015) Classification of Alzheimer's disease from quadratic sample entropy of electroencephalogram. *Healthc Technol Lett* **2**, 70-73.

[52] Houmani N, Dreyfus G, Vialatte FB (2015) Epoch-based entropy for early screening of Alzheimer's disease. *Int J Neural Syst* **25**, 1550032.

[53] Ahmadlou M, Adeli H, Adeli A (2011) Fractality and a wavelet-chaos-methodology for EEG-based diagnosis of Alzheimer disease. *Alzheimer Dis Assoc Disord* **25**, 85-92.